International Forum on Aeroelasticity and Structural Dynamics
IFASD 2017
25-28 June 2017 Como, Italy

AN OPTIMIZED DOUBLET-LATTICE METHOD CORRECTION APPROACH FOR A LARGE CIVIL AIRCRAFT

C. Valente[1], C. Wales[1], D. Jones[1], A. Gaitonde[1], J. E. Cooper[1], Y. Lemmens[2]

[1]Department of Aerospace Engineering
University of Bristol
Queens Building, University Walk, Bristol BS8 1TR UK
carmine.valente@bristol.ac.uk

[2]Siemens Industry Software NV
Interleuvenlaan 68 Leuven 3001 Belgium

Keywords: Aeroelasticity, CFD, Fluid Structure Interaction, Structural Dynamics, Gust

Abstract: This paper presents an efficient correction technique for doublet-lattice method, where linearized frequency domain analysis have been used to compute the aerodynamic data for the corrections. This substantially reduces the computational cost necessary to define the corrected Aerodynamic Interference Coefficients matrices. The results obtained from the corrected doublet-lattice method are compared to the fully coupled CFD/FEM solution performed using the Alpes Fluid Structure Interaction Interface. The application of this method to two test cases, representative of civil jet airliner in cruise condition, in transonic regime, is presented. The first test case is an Euler simulation for the FFAST right wing model, while the second presents preliminary results obtained using a viscous simulation for the NASA common research model. The aeroelastic loads analysis for three different gust lengths, as prescribed by the CS-25, are presented and discussed.

1 INTRODUCTION

The current industrial standard for gust loads modelling is to use traditional potential flow models, such as the doublet-lattice method (DLM) and strip theory [1, 2], to generate the air loads interacting with the aircraft structure. However the growing interest in flexible-aircraft dynamics has highlighted how these models make simplifying assumptions that may not allow an accurate prediction of the air loads in these cases. Since linear unsteady aerodynamics show inaccuracies in the transonic regime, where the linear assumptions are no longer valid and the effects of viscosity and thickness are relevant, many correction techniques have been developed in the past years [3,4] to attempt to address this issue. Their aim is to introduce wind tunnel data and Computational Fluid Dynamics (CFD) results into the linear unsteady aerodynamics [5, 6] to give improved predictions in this flight regime. Unfortunately most of them rely on a large quantity of additional data. The increased availability of high performance computing, has seen the development of reliable fluid and structural solvers for use in the engineering design process [7–9]. In particular in the aeroelastic domain, fluid structure interaction procedures are often considered as a means of replacing expensive experimental campaigns. However, they are too expensive to be used as only way to cover the entire loads design process.

For many years the doublet-lattice method has been used as the reference method in the aerospace industry to compute unsteady aerodynamics. One of the main advantages that it offers is the low computational cost and the integration in the commercial aeroelastic solver Nastran. So, it has become the standard method to compute the aerodynamic loads interacting with the structure for gust analysis. However being based on the linearized potential equations, it doesn't describe effects related to thickness, shock wave formation or viscosity.

The idea of using a correction technique is to combine the cheap computational cost of a lower order method, with the information obtained with an higher order method, achieving a good compromise between performance and accuracy. This make possible the investigation of thousand of loads cases, necessary for flutter and dynamic flight loads, approximating the complex flow effects. Several techniques have been presented during the last decades to correct the aerodynamic coefficient influence matrix $AICs$. In particular, the industrial approach has been to match the steady results at zero frequency. The common idea, at the base of most of these correction methods, is to use non-linear pressure distribution measured on the model, or computed with CFD analysis, to correct the result obtained from linear methods. In the last years reduced order models have become very popular, and new methods to perform Linearized Frequency Domain (LFD) analysis have been introduced [10–12]. Nonetheless these approaches often require a very high number of simulations to build these models.

The work presented in this paper defines a new approach to correct the air loads computed using the doublet-lattice method for gust loads analysis [13]. This method has been formulated in the frequency domain and calculates a correction at selected frequencies. It makes use of a post multiplying approach, and considers complex correction factors to ensure a good representation of the unsteady aerodynamics. Linear Frequency Domain analysis has been used to reduce the computational cost necessary to evaluate the reference aerodynamics loads. Additionally an interpolation method over the correction factor, can be performed to reduce the number of reference case to analyse in the LFD code. In the implementation of the method a strip loads approach is used to evaluate the reference aerodynamics loads, based on the consideration that a good representation of the shock position and movement is not achievable mainly due to the low refinements in the aerodynamic panel discretization.

2 DOUBLET-LATTICE METHOD CORRECTION APPROACH

The aeroelastic frequency response analysis in modal coordinates, as implemented in the Nastran solver, is based on the solution of the following equation:

$$\left[-\omega^2\mathbf{M}_{hh} + i\omega\mathbf{B}_{hh} + (1+ig)\,\mathbf{K}_{hh} - \bar{q}\mathbf{Q}_{hh}(M,k)\right]\mathbf{U}_h = \bar{q}w_g\mathbf{PP}(\omega)\mathbf{Q}_{hj}(M,k)\mathbf{w}_j(\omega) \quad (1)$$

where two are the terms that account for the aerodynamic loads. The first due to a structural deformation:

$$\mathbf{Q}_{hh}(M,k) = \boldsymbol{\phi}_{ah}^T\mathbf{G}_{ka}^T\mathbf{S}_{kj}\ \mathbf{A}_{jj}^{-1}\ \mathbf{D}_{jk}\mathbf{G}_{ka}\boldsymbol{\phi}_{ah} \quad (2)$$

and the second due to a gust disturbance :

$$\mathbf{Q}_{hj}(M,k) = \boldsymbol{\phi}_{ah}^T\mathbf{G}_{ka}^T\mathbf{S}_{kj}\ \mathbf{A}_{jj}^{-1} \quad (3)$$

These two contribution are linearly added to evaluate the total aerodynamic loads. For this reason, the presented correction method corrects first the rigid gust loads and then the aerodynamic load obtained from a mode shape deformation.

2.1 AICs Correction using Sinusoidal Gusts

The aim of this correction approach is to match the integrated aerodynamic loads acting on the structural nodes computed from the CFD code for a sinusoidal gust shape:

$$\mathbf{F}_a^{CFD_G} = \widehat{\mathbf{F}}_a^{DLM_G} \tag{4}$$

where the right hand side term can be expanded for the corrected Doublet Lattice Method [14], as follow:

$$\mathbf{F}_a^{CFD_G} = \bar{q} w_g \mathbf{PP}(\omega) \mathbf{G}_{kr}^T \mathbf{S}_{kj}\ \mathbf{A}_{jj}^{-1} \mathbf{W}_{jj}^w \mathbf{w}_j(\omega) \tag{5}$$

where:

$\bar{q}$ dynamic pressure
w_g gust scaling factor
$\mathbf{PP}(\omega)$ Fourier transform of the time domain gust disturbance defined by the user
$\mathbf{G}_{kr}^T$ integration matrix over the aerodynamic monitor points
$\mathbf{S}_{kj}$ aerodynamic integration matrix
$\mathbf{A}_{jj}$ aerodynamic influence coefficient matrix, $AICs$
$\mathbf{W}_{jj}^w$ correction coefficients matrix
$\mathbf{w}_j$ downwash matrix

The downwash contribution is a matrix defined as follow

$$\mathbf{w}_j(\omega_i) = \cos\gamma_j e^{-i\omega_i (x_j - x_0)/U_\infty} \qquad \text{with } i = 1, \cdots, N_f \tag{6}$$

where:

ω_i excitation frequency, or gust frequency
γ_j dihedral angle of the j-th aerodynamic element
x_j x-location of the j-th aerodynamic element in the aerodynamic coordinate system
x_0 reference coordinate for the gust

The correction process aims to find the matrices $\mathbf{W}_{jj}^w$ such that the sectional loads computed with the DLM method match the CFD loads. There is not a unique matrix that can be used to correct the DLM, so the idea is to find a matrix that minimise the change to the DLM solution. The aim is to find a matrix $\mathbf{W}_{jj}^w$ as close to the identity matrix as possible. This means minimising the weighted sum of the square of the deviations, where the deviation $\mathbf{W}_{jj}^w$ is defined as the difference between the correction factor and unity

$$\mathbf{W}_{jj}^w = \begin{bmatrix} \ddots & & \\ & \mathbf{I} + \boldsymbol{\epsilon}^w & \\ & & \ddots \end{bmatrix} \tag{7}$$

Defining the generalized aerodynamic influence coefficient matrix relating the downwash to the aerodynamic loads on the monitor points, which correspond to the CFD strips being matched:

$$\mathbf{QARJ}^T = \mathbf{G}_{kr}^T \mathbf{S}_{kj}\ \mathbf{A}_{jj}^{-1} \tag{8}$$

it is possible to rewrite

$$\mathbf{F}_a^{CFD_G} = \bar{q} w_g \mathbf{PP}(\omega) \mathbf{QARJ}^T \mathbf{W}_{jj}^w \mathbf{w}_j(\omega) \tag{9}$$

Considering a time gust disturbance with a sinusoidal shape, the Fourier Transform comes to be a vector with only one non zero component, corresponding to the frequency of the input signal. Expanding Eq. 9 for a single frequency, it is a possible to write:

$$\mathbf{F}_a^{CFD_G} = \bar{q} w_g \mathbf{QARJ}^T \mathbf{W}_{jj}^w \bar{\mathbf{w}}_j^G \tag{10}$$

Considering a diagonal correction matrix Eq. (10) can be written as:

$$\mathbf{F}_a^{CFD_G} = \mathbf{F}_a^{DLM_G} + \bar{q} w_g \mathbf{QARJ}^T \begin{bmatrix} \ddots & & \\ & \boldsymbol{\epsilon}^w & \\ & & \ddots \end{bmatrix} \bar{\mathbf{w}}_j^G \tag{11}$$

defining $\Delta\mathbf{F}_a^G$ as the difference between the high fidelity simulations and the uncorrected DLM loads:

$$\Delta\mathbf{F}_a^G = \mathbf{F}_a^{CFD_G} - \mathbf{F}_a^{DLM_G} \tag{12}$$

it is possible to express the change in aerodynamic loads as:

$$\Delta\mathbf{F}_a^G = \bar{q} w_g \mathbf{QARJ}^T \begin{bmatrix} \ddots & & \\ & \bar{\mathbf{w}}_j^G & \\ & & \ddots \end{bmatrix} \{\boldsymbol{\epsilon}^w\} \tag{13}$$

Introducing the following matrix:

$$\mathbf{QP} = w_g \mathbf{QARJ}^T \begin{bmatrix} \ddots & & \\ & \bar{\mathbf{w}}_j^G & \\ & & \ddots \end{bmatrix} \tag{14}$$

Eq. (13) becomes:

$$\Delta\mathbf{F}_a^G = \bar{q}\mathbf{QP}\{\boldsymbol{\epsilon}^w\} \tag{15}$$

All the matrices and vectors in Eq. (15) are complex, so it possible to rewrite it as:

$$\Re(\Delta\mathbf{F}_a^G) + i\Im(\Delta\mathbf{F}_a^G) = \bar{q}[\Re(\mathbf{QP}) + i\Im(\mathbf{QP})]\{\Re(\boldsymbol{\epsilon}^w) + i\Im(\boldsymbol{\epsilon}^w)\} \tag{16}$$

Using the following notation:

$$\begin{aligned} \Re(\Delta\mathbf{F}_a^G) &= \Delta\mathbf{F}_a{}^{R^G} \\ \Im(\Delta\mathbf{F}_a^G) &= \Delta\mathbf{F}_a{}^{I^G} \\ \Re(\mathbf{QP}) &= \mathbf{QP}^R \\ \Im(\mathbf{QP}) &= \mathbf{QP}^I \\ \Re(\boldsymbol{\epsilon}^w) &= \boldsymbol{\epsilon}^R \\ \Im(\boldsymbol{\epsilon}^w) &= \boldsymbol{\epsilon}^I \end{aligned} \tag{17}$$

it is possible to write Eq. (16) as:

$$\begin{aligned} \Delta\mathbf{F}_a^{R^G} + i\Delta\mathbf{F}_a^{I^G} &= \bar{q}\Big(\mathbf{QP}^R + i\mathbf{QP}^I\Big)\Big(\boldsymbol{\epsilon}^R + i\boldsymbol{\epsilon}^I\Big) \\ &= \bar{q}\Big(\mathbf{QP}^R\boldsymbol{\epsilon}^R + i\mathbf{QP}^R\boldsymbol{\epsilon}^I + i\mathbf{QP}^I\boldsymbol{\epsilon}^R - \mathbf{QP}^I\boldsymbol{\epsilon}^I\Big) \end{aligned} \tag{18}$$

and writing it in a matrix format, it is possible to obtain:

$$\begin{Bmatrix} \Delta\mathbf{F}_a^{R^G} \\ \Delta\mathbf{F}_a^{I^G} \end{Bmatrix} = \bar{q} \begin{bmatrix} \mathbf{QP}^R & -\mathbf{QP}^I \\ \mathbf{QP}^I & \mathbf{QP}^R \end{bmatrix} \begin{Bmatrix} \boldsymbol{\epsilon}^R \\ \boldsymbol{\epsilon}^I \end{Bmatrix} \tag{19}$$

Solving in a least square sense it is possible to determine the correction factors and obtain the correction matrix for each reduced frequency.

2.2 AICs Correction using Harmonic Mode Shape Deformations

The aerodynamic strip loads due to an harmonic mode deformation of the structure, in the frequency domain, calculated using the DLM can be expressed as:

$$\mathbf{F}_a^{DLM_{MS}} = \bar{q}\mathbf{G}_{kr}^T\mathbf{S}_{kj}\ \mathbf{A}_{jj}^{-1}\mathbf{w}_{ja}^{MS} \tag{20}$$

where the downwash due to the mode shape deformation is given by:

$$\mathbf{w}_{ja}^{MS} = (\mathbf{D}_{jk}^1 + ik\mathbf{D}_{jk}^2)\mathbf{G}_{ka}^T\tilde{\mathbf{u}}_a \tag{21}$$

where $\tilde{\mathbf{u}}_a$ is the Fourier transform of the structural mode deformation time history, given by the product of the mode amplitude and a vector defining the time history of the harmonic shape variation:

$$\tilde{\mathbf{u}}_a = \mathcal{F}(\mathbf{u}_a(t)) \tag{22}$$

Using the same approach as the gust correction we can introduce a correction matrix to match the mode shape loads calculated with CFD, leading to the equation:

$$\mathbf{F}_a^{CFD_{MS}} = \bar{q}\mathbf{G}_{kr}^T\mathbf{S}_{kj}\ \mathbf{A}_{jj}^{-1}\mathbf{W}_{jj}^{w}\mathbf{w}_{ja}^{MS} \tag{23}$$

Using Eq. (8) it is possible to rewrite Eq. (23) as:

$$\mathbf{F}_a^{CFD_{MS}} = \bar{q}\mathbf{QARJ}^T\mathbf{W}_{jj}^{w}\mathbf{w}_{ja}^{MS} \tag{24}$$

and using a diagonal definition for $\mathbf{W}_{jj}^{w}$ as done in Eq. (7), the delta aerodynamic loads can be expressed as:

$$\Delta\mathbf{F}_a^{MS} = \mathbf{F}_a^{CFD_{MS}} - \mathbf{F}_a^{DLM_{MS}} \tag{25}$$

$$\Delta\mathbf{F}_a^{MS} = \bar{q}\mathbf{QARJ}^T \begin{bmatrix} \ddots & & \\ & \boldsymbol{\epsilon}^w & \\ & & \ddots \end{bmatrix} \{\mathbf{w}_{ja}^{MS}\} = \bar{q}\mathbf{QARJ}^T \begin{bmatrix} \ddots & & \\ & \mathbf{w}_{ja}^{MS} & \\ & & \ddots \end{bmatrix} \{\boldsymbol{\epsilon}^w\} \tag{26}$$

introducing the matrix:

$$\mathbf{QW} = \mathbf{QARJ}^T \begin{bmatrix} \ddots & & \\ & \mathbf{w}_{ja}^{MS} & \\ & & \ddots \end{bmatrix} \tag{27}$$

it is possible to write:

$$\Delta\mathbf{F}_a^{MS} = \bar{q}\mathbf{QW}\{\boldsymbol{\epsilon}^w\} \tag{28}$$

Proceeding in an analogues way to what is done in Eq.(16), introducing the notation:

$$\begin{aligned} \Re(\mathbf{QW}) &= \mathbf{QW}^R \\ \Im(\mathbf{QW}) &= \mathbf{QW}^I \end{aligned} \tag{29}$$

Eq. 28 can be expressed as:

$$\Delta\mathbf{F}_a^{R^{MS}} + i\Delta\mathbf{F}_a^{I^{MS}} = \bar{q}\Big(\mathbf{QW}^R\boldsymbol{\epsilon}^R + i\mathbf{QW}^R\boldsymbol{\epsilon}^I + i\mathbf{QW}^I\boldsymbol{\epsilon}^R - \mathbf{QW}^I\boldsymbol{\epsilon}^I\Big) \tag{30}$$

$$\begin{Bmatrix} \Delta\mathbf{F}_a^{R^{MS}} \\ \Delta\mathbf{F}_a^{I^{MS}} \end{Bmatrix} = \bar{q} \begin{bmatrix} \mathbf{QW}^R & -\mathbf{QW}^I \\ \mathbf{QW}^I & \mathbf{QW}^R \end{bmatrix} \begin{Bmatrix} \boldsymbol{\epsilon}^R \\ \boldsymbol{\epsilon}^I \end{Bmatrix} \tag{31}$$

In this case only one mode has been considered, but the system can be extended to additional mode shapes deformation. As seen before, the least square solution of this system gives the correction factors necessary to evaluate the correction matrix for each reduced frequency.

3 CORRECTION METHOD APPLICATION

Two applications of the correction method are presented in the following sections. At first a comparison using the FFAST right wing model, considering an Euler simulation, is carried out. Afterwards the method is applied to the NASA common research model using a RANS CFD simulation.

3.1 Aeroelastic response to discrete gust

The correction factors computed as described in the previous section, have been used to evaluate the $AICs$ matrices computed by Nastran in the solution sequence for frequency response analysis. The corrected matrices are saved in a ".OP4" format and replaced at running time to the ones computed by Nastran. The gust response to a "1-COS" discrete gust shape has been studied for three different gust lengths. The shape of the gust has been defined considering the "Certification Specification for Large Aeroplanes CS-25" [15], using the following equation:

$$W_g(x) = \begin{cases} \frac{U_{ds}}{2}\left(1 - cos\left(\frac{\pi x}{H}\right)\right) & for\ \ 0 \leq x \leq 2H \\ \\ 0 & otherwise \end{cases} \tag{32}$$

where x is the distance penetrated into the gust, U_{ds} is the design gust velocity in equivalent air speed (EAS), defined by Eq. (33), and H (in m) is the distance parallel to the flight path of the aeroplane for the gust to reach its peak velocity ($H = L_g/2$, half of the gust wavelength). The design gust velocity is then defined as:

$$U_{ds} = U_{ref} F_g \left(\frac{H}{106.68}\right)^{1/6} \tag{33}$$

where U_{ref} is the reference gust velocity in EAS and F_g is the load alleviation factor.

3.2 FFAST right wing test case

A full aircraft beam stick FE model with lumped masses, representative of a single-aisle civil jet airliner, was developed as part of the FFAST project [16]. From this, the right wing model has been extracted and considered clamped at the root, Figure 1.

The FFAST right wing FE model contains 10 beam elements for a total of 11 structural grid points, while the aerodynamic panel model counts of 11 boxes in the chord wise direction and 45 boxes in span, for a total of 495 aerodynamic panels. The panel method used in this investigation is the doublet-lattice method available in the commercial solver Nastran.

The wing CFD model (created using aerofoil data available for the three sections: root, crank and tip) does not include the engine and pylon, and has 33227 surface grid points, Figure 1(a). The CFD model has been solved using Euler equations considering a reference flight condition at $1g$, an altitude of $11000\ m$ and Mach number of $M = 0.85$. High fidelity aeroelastic data have been computed using a Fluid Structure Interaction (FSI) interface, called AlpesFSI [17]. This interface provides a means to combine the finite element analysis with the loads computed from an external computational fluid dynamic (CFD) solver. In the current case the CFD code chosen has been the DLR TAU-code [18]. The gust is modelled in TAU using a field velocity method

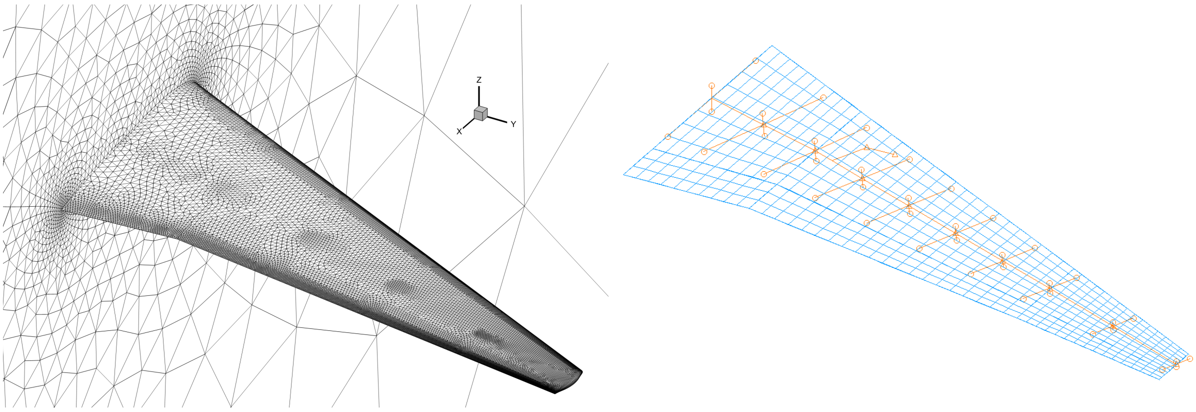

(a) FFAST right wing CFD model.

(b) FFAST right wing FE and DLM model.

Figure 1: FFAST right wing aerodynamic and structural model.

(FVM) [19–21]. It is prescribed to start just outside the computational domain and travel at free stream velocity U_∞. The AlpesFSI interface has been used to identify the aeroelastic trim deformation, from which an unsteady gust response analysis has been performed. In order to fit the strip loads approach, discussed in the previous sections, both the DLM and CFD meshes have been divided into ten strips along the span (starting with the first strip at the root of the wing). Each strip is defined around a structural grid node as shown in Figure 2. The integrated loads computed from the CFD analysis, for each strip, is used as the target loads that the low fidelity method should be able to predict.

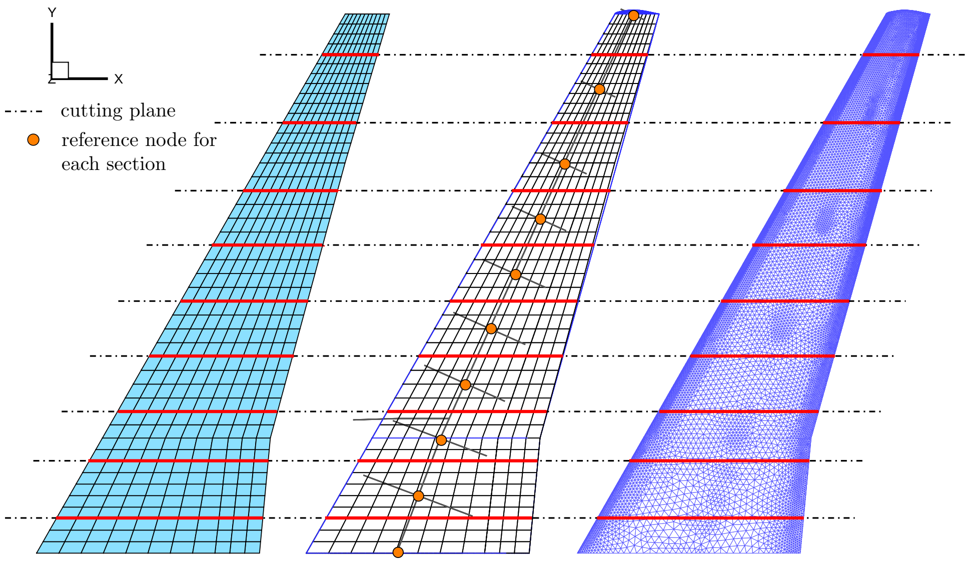

Figure 2: Comparison of DLM and CFD mesh, showing the sectional cutting planes and structural nodes along the wing aperture.

The correction method described in the present work has been intended to use Linear Frequency Domain Analysis (LFD) [11, 12] to evaluate the reference data for the correction. Initially the high fidelity aeroelastic simulations have been performed in the time domain. So a comparison of the time domain and LFD solutions has been performed. First the two methods were compared considering the rigid wing encountering sinusoidal gust at different wavelength.

To remain in the linear region a small gust amplitude, equivalent to a $\alpha_g = 0.25°$, has been chosen. Different gust lengths have been considered to match different reduced frequencies:

$$k = \frac{\omega_g}{U_\infty}\frac{l_{ref}}{2} = \frac{2\pi f_g}{U_\infty}\frac{l_{ref}}{2} \tag{34}$$

where the gust frequency f_g is dependent on the gust length:

$$f_g = \frac{U_{inf}}{L_g} \tag{35}$$

A range of reduced frequency between $k = 0.01$ and $k = 2.0$, has been considered in the gust simulation performed in the frequency domain. The comparison between CFD and LFD is reported for three different strips along the span in Figure 3.

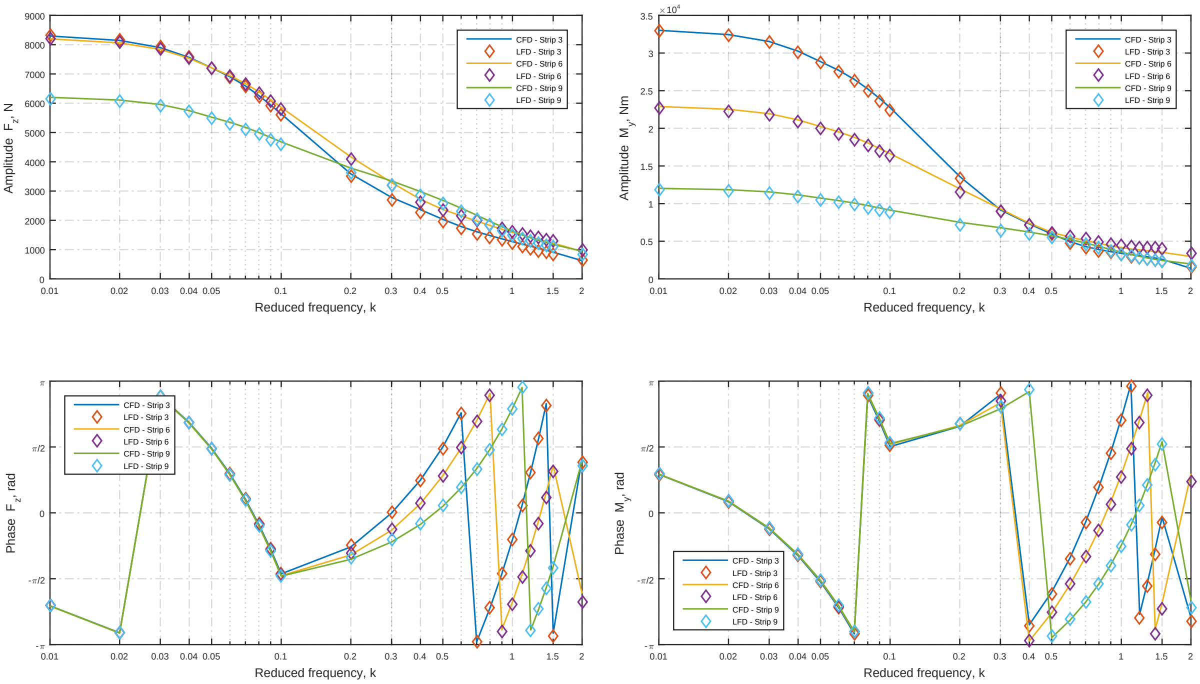

(a) Vertical force, F_z.

(b) Pitching moment, M_y.

Figure 3: Amplitude and phase comparison versus reduced frequency due to sinusoidal gust encountering for CFD and LFD. Vertical force and pitching moment for strip 3, 6 and 9.

Two different flexible mode shapes have been considered to evaluate the flexible loads contribution, Figure 4. The first wing bending and first wing torsion have been mapped into the CFD model, and LFD analysis have been considered for the range of reduced frequency mentioned. A small amplitude has been considered for the mode deformation: a maximum displacement at the wing tip of 10 and 5 cm has been considered respectively, for the first and second mode. A comparison between CFD and LFD results for the strip vertical force and pitching moment has been reported in Figure 5 for the first mode and in Figure 6 for the second mode.

As it is possible to check in Figure 3, 5 and 6 a good agreement between the full time domain analysis and the linearised frequency approach has been found.

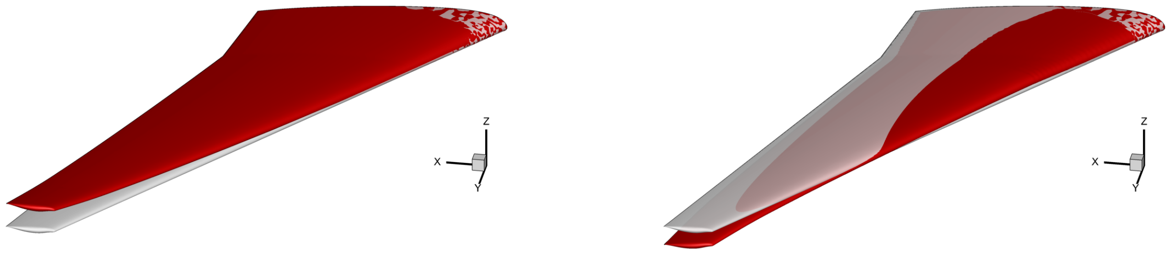

(a) First wing bending.

(b) First wing torsion

Figure 4: Mode shapes of FFAST wing mapped to CFD surface mesh.

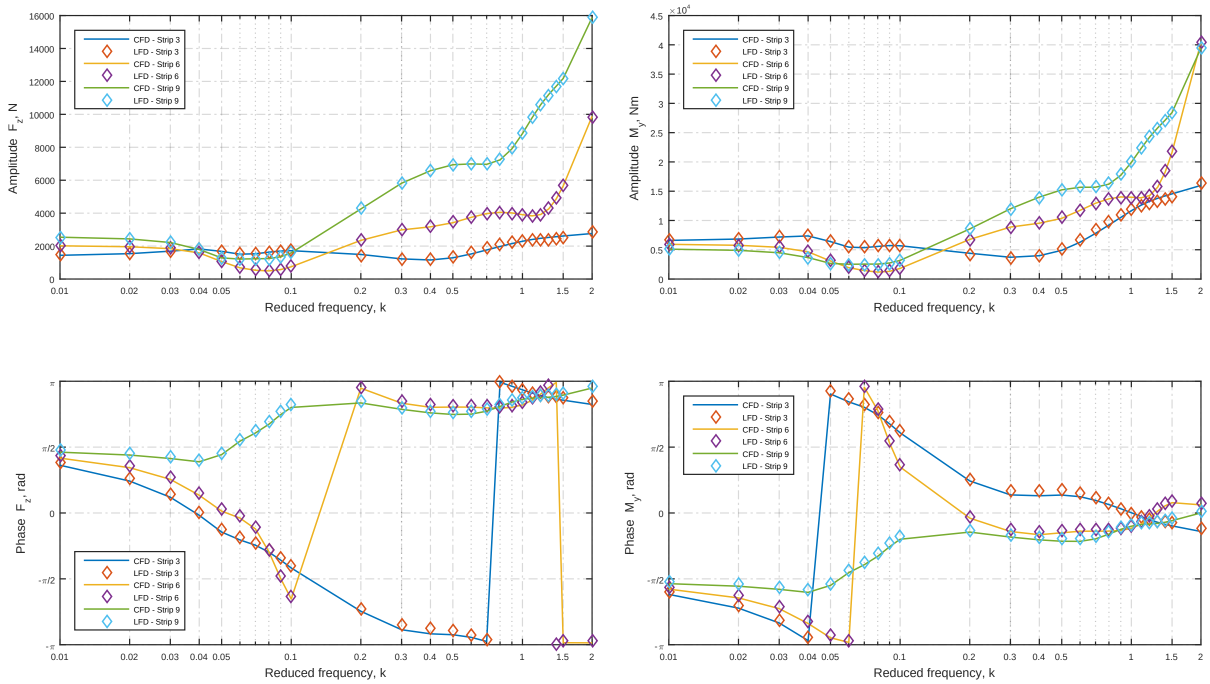

(a) Vertical force, F_z

(b) Pitching moment, M_y.

Figure 5: Amplitude and phase comparison versus reduced frequency due to first wing bending harmonic deformation for CFD and LFD. Vertical force and pitching moment for strip 3, 6 and 9

For the discrete gust loads analysis three gust lengths have been analysed, considering a gust alleviation factor value F_g equal to 1. Table 1 reports the gust profiles properties used in the investigation.

$AoA,\ deg$	$L_g,\ m$	$W_g^{TAS},\ m/s$	M	$\alpha_g,\ deg$	$T_g,\ sec$
0.0	18.28	12.29	0.85	2.81	0.073
0.0	91.44	16.07	0.85	3.67	0.365
0.0	213.36	18.51	0.85	4.22	0.851

Table 1: "1-COS" gust profiles considered for the FFAST right wing test case.

The results comparing the total vertical force and pitching moment have been reported in Figure 7. In these plots only the delta loads, removing the steady aeroelastic loads at trim, is shown. Since the time domains and LFD analysis are in perfect agreement the correction of the DLM model using both methods matches perfectly. Considering only the rigid gust contribution is not

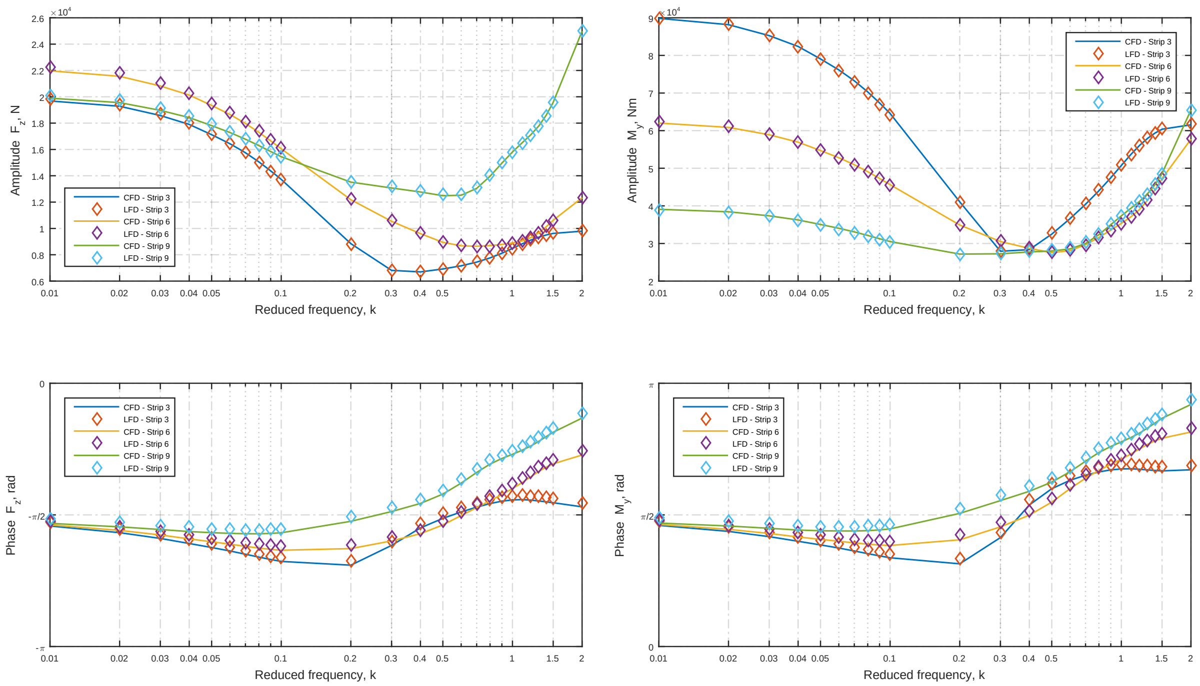

(a) Vertical force, F_z (b) Pitching moment, M_y.

Figure 6: Amplitude and phase comparison versus reduced frequency due to the first wing torsion harmonic deformation for CFD and LFD. Vertical force and pitching moment for strip 3, 6 and 9

enough to achieve a good correction of the total aeroelastic loads, for this reason it is important to consider a correction on the flexible mode shape deformation as well, as shown in a previous work of the authors [13]. As it is possible to notice the corrected panel method matches very well the fully coupled results for the short and medium gust length. However for the long gust length the corrected DLM method tends to shift a bit from the desired solution. This behaviour is due to the non-linear effects that the correction approach does not consider in the present formulation. Nevertheless it is evident how the correction proposed can capture the right dynamic behaviour predicted by the FEM/CFD coupled solution.

3.3 Aeroelastic model NASA common research model

A second test case has been considered to check the behaviour of the correction method in presence of viscous effect. The NASA common research model (NCRM) is used in the wing body and tail configuration from the 4th drag prediction workshop [22]. For the structural model the FERMAT FEM [23] for maximum take-off weight case was used. The reference flight aero geometry from the 4th drag prediction workshop [22] was used as the aeroelastic flight shape for Test Case H. All simulations were performed using the negative Spalart-Allmaras turbulence model [24]. The simulations were carried out using the coarse solar mesh submitted by DLR to the 4th drag prediction workshop [25]. A new doublet-lattice mesh has been created, including the fuselage and a comparison of the CFD and DLM model is shown in Figure 8.

At the time of publication only rigid gust results are available for this application, so no flexible effect are discussed, but they are under investigation and will be presented in future works. Details of the “1-COS” gust profiles investigated are given in Table 2. A reference cruise flight condition at $1g$, altitude of $9142\ m$ and Mach number of 0.86 is considered. The total wing vertical forces and pitching moments are plotted for the different gust lengths in Figure 9.

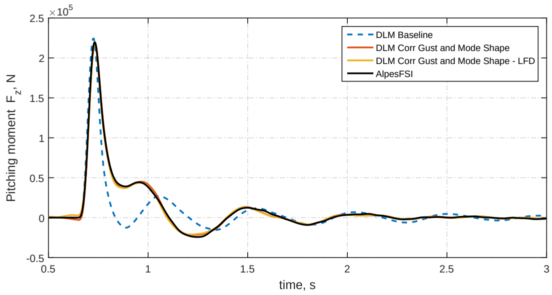

(a) Vertical force F_z, $L_g = 18\ m$.

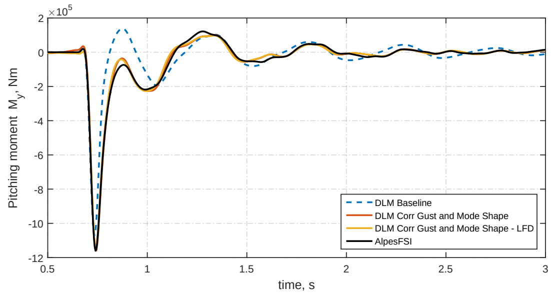

(b) Pitching moment M_y, $L_g = 18\ m$.

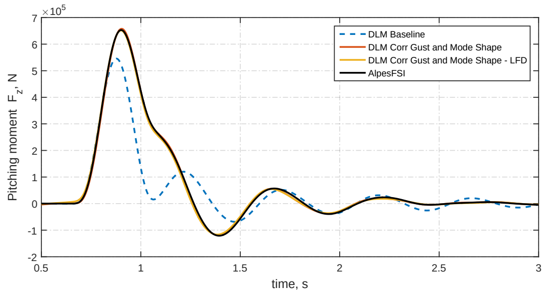

(c) Vertical force F_z, $L_g = 91\ m$.

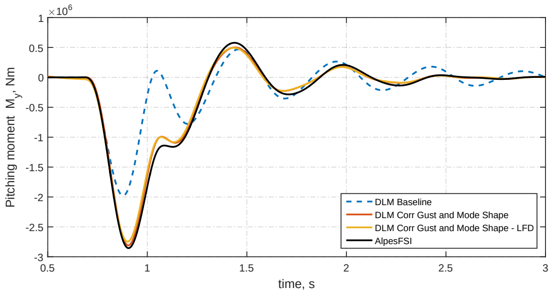

(d) Pitching moment M_y, $L_g = 91\ m$.

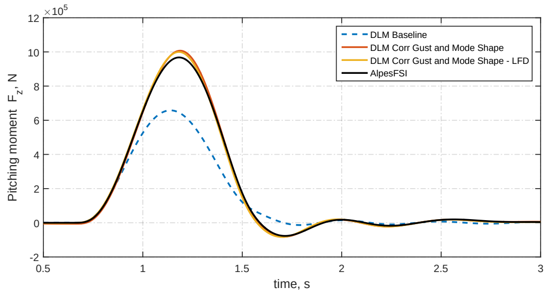

(e) Vertical force F_z, $L_g = 213\ m$.

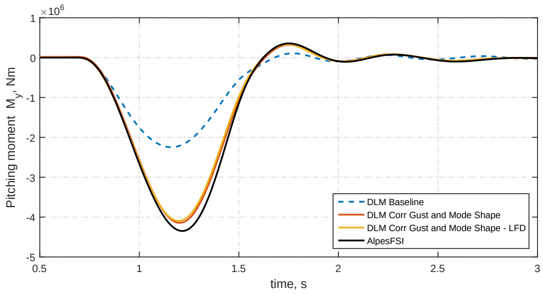

(f) Pitching moment M_y, $L_g = 213\ m$.

Figure 7: Comparison of vertical force and pitching moment computed with Baseline DLM, Corrected DLM and AlpesFSI interface, for the FFAST right wing.

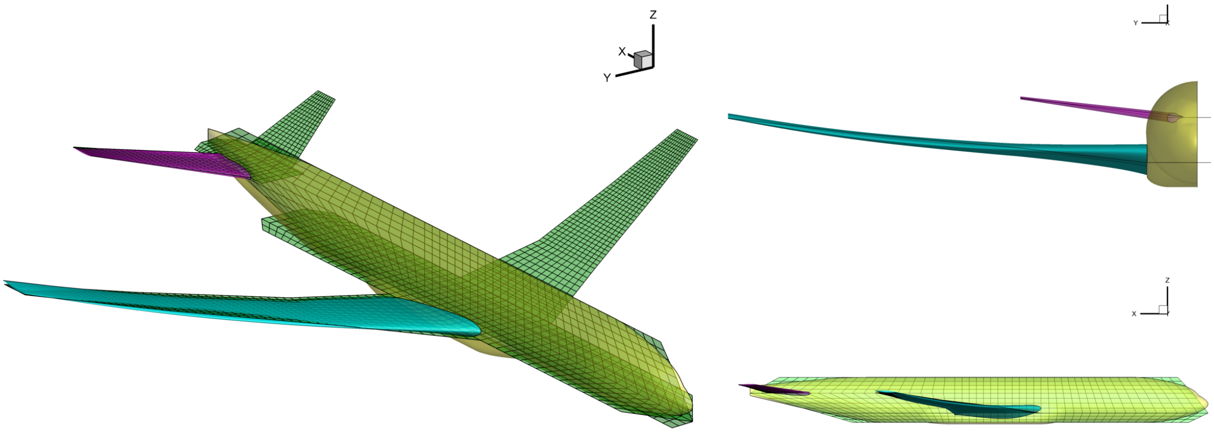

Figure 8: Comparison of DLM and CFD mesh for Nasa Common Research Model.

$AoA,\ deg$	$L_g,\ m$	$W_g^{TAS},\ m/s$	M	$\alpha_g,\ deg$	$T_g,\ sec$
0.0	18.28	11.24	0.86	2.46	0.070
0.0	91.44	14.70	0.86	3.22	0.350
0.0	213.36	16.94	0.86	3.71	0.818

Table 2: “‘1-COS” gust profiles considered for the NASA common research model.

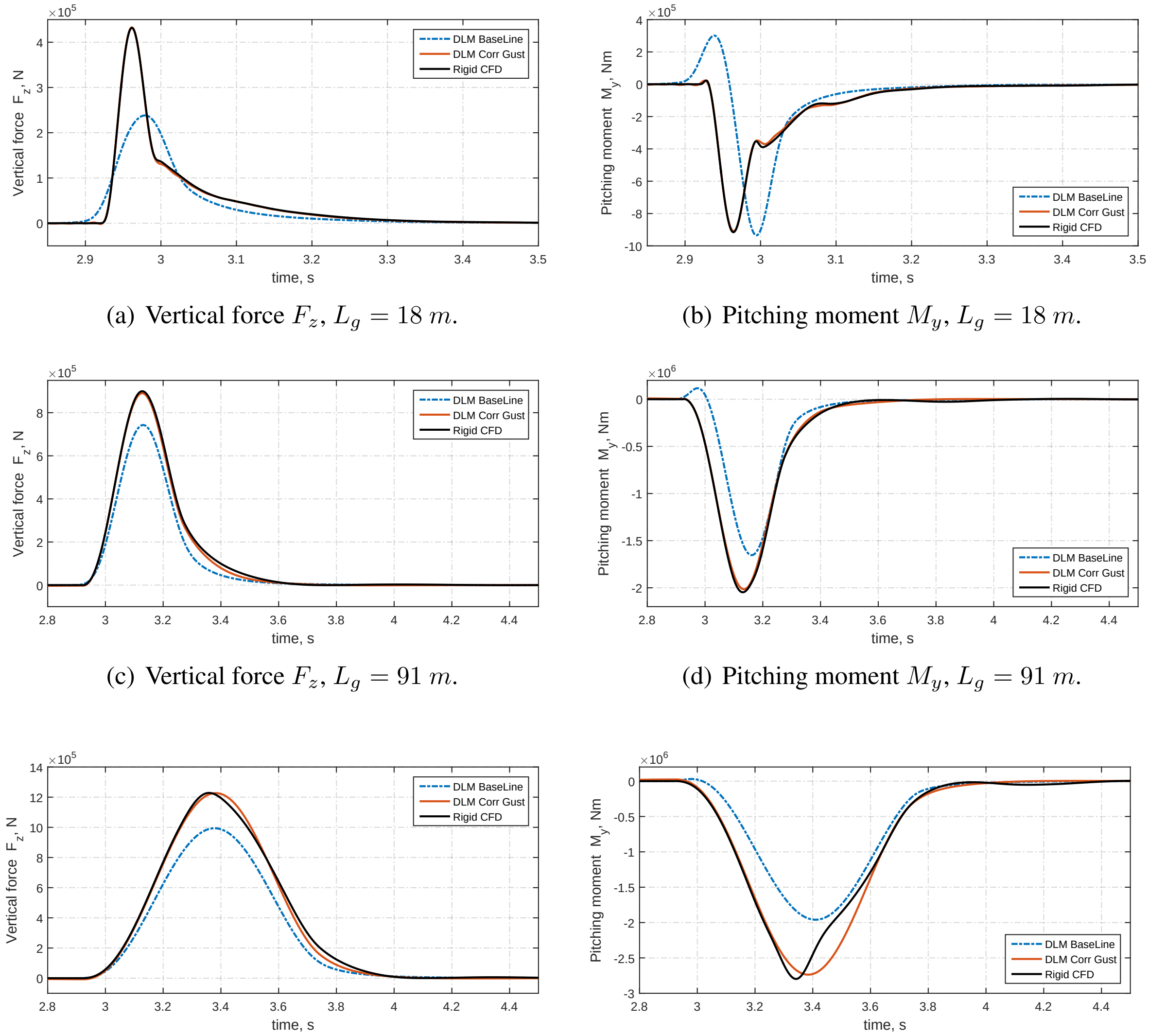

(a) Vertical force F_z, $L_g = 18\ m$.

(b) Pitching moment M_y, $L_g = 18\ m$.

(c) Vertical force F_z, $L_g = 91\ m$.

(d) Pitching moment M_y, $L_g = 91\ m$.

(e) Vertical force F_z, $L_g = 213\ m$.

(f) Pitching moment M_y, $L_g = 213\ m$.

Figure 9: Comparison of vertical force and pitching moment computed with Baseline DLM, Corrected DLM rigid CFD, for the NASA common research model.

The correction approach using LFD for sinusoidal gust is able to produce a good approximation of the gust loads for the short and medium gust length. However for the longest gust case non-linear effect become relevant and the correction method, based on linear assumptions, shows a slightly difference from the CFD analysis.

4 CONCLUSION

A new methodology to correct the Doublet-lattice method has been presented. The proposed approach is capable to take full advantage of the linearised frequency domain analysis available in the DLR TAU code, providing an efficient way to compute the reference high fidelity loads necessary to evaluate the correction coefficients. However, in presence of very flexible structure, non-linear effects can become relevant and the assumption of super imposition of effects, on which the method is based, can start to produce a lack of accuracy respect to the fully coupled CFD/FEM solution. On going activities are investigating how to account the non linear behaviour due to the coupling of aeroelastic effects in transonic regime.

5 ACKNOWLEDGMENTS

The research leading to these results has received funding from the European Community's Marie Curie Initial Training Network (ITN) on Aircraft Loads Prediction using Enhanced Simulation (ALPES) FP7-PEOPLE-ITN-GA-2013-607911. The partners in the ALPES ITN are the University of Bristol, Siemens and Airbus Operations Ltd.

This work was carried out using the computational facilities of the Advanced Computing Research Centre, University of Bristol - http://www.bris.ac.uk/acrc/.

6 REFERENCES

[1] Albano, E. and Rodden, W. P. (1969). A Doublet-Lattice Method for Calculating Lift Distributions on Oscillating Surfaces in Subsonic Flows. *AIAA Journal*, 7(2), 279–285.

[2] Rodden, W. P. and Taylor, P. F. Improvements To the Doublet-Lattice Method in MSC Nastran, 1–16.

[3] Rodden, W. P., Taylor, P. F., and McIntosh, S. C. (1998). Further Refinement of the Subsonic Doublet-Lattice Method. *Journal of Aircraft*, 35(5), 720–727. ISSN 0021-8669. doi:10.2514/2.2382.

[4] Palacios, R., Climent, H., Karlsson, A., et al. (2001). Assessment of strategies for correcting linear unsteady aerodynamics using CFD or experimental results. In *International Forum on Aeroelasticity and Structural Dynamics (IFASD)*.

[5] Giesing, J. P., Kalman, T. P., and Rodden, W. P. (1976). Correction Factor Techniques for Improving Aerodynamic Prediction Methods.

[6] Brink-Spalink, J. and Bruns, J. M. (2000). Correction of unsteady aerodynamic influence coefficients using experimental or CFD data. In *41st AIAA Conference Atlanta, GA*.

[7] Heinrich, R. and Kroll, N. (2008). Fluid-Structure Coupling for Aerodynamic Analysis and Design A DLR Perspective. *Most*, (January), 1–31. doi:10.2514/6.2008-561.

[8] Keye, S. (2009). Fluid-Structure-Coupled Analysis of a Transport Aircraft and Comparison to Flight Data. In *39th AIAA Fluid Dynaminamics Conference*, 22-25 June 2009. San Antonio, Texas. ISBN 9781563479755, pp. 1–10.

[9] Stickan, B., Bleecke, H., and Schulze, S. (2013). NASTRAN Based Static CFD-CSM Coupling in FlowSimulator. *Computational Flight Testing Notes on Numerical Fluid Mechanics and Multidisciplinary Design*, 123, 223–234.

[10] Timme, S., Badcock, K. J., and Ronch, a. D. (2013). Linear Reduced Order Modelling for Gust Response Analysis Using the DLR-TAU Code. In *IFASD 2013 International Forum on Aeroelasticity and Structural Dynamics*. Bristol, U.K.

[11] Bekemeyer, P. and Timme, S. (2016). Reduced Order Gust Response Simulation using Computational Fluid Dynamics. In *57th AIAA/ASCE/AHS/ASC Structures, Structural Dynamics, and Materials Conference*, January. San Diego, California, USA, pp. 1–13. doi:10.2514/6.2016-1485.

[12] Bekemeyer, P., Thormann, R., and Timme, S. (2016). Rapid Gust Response Simulation of Large Civil Aircraft using Computational Fluid Dynamics. In *Applied Aerodynamics Conference*, 19-21 July 2016. Bristol, UK, pp. 1–12.

[13] Valente, C., Wales, C., Jones, D., et al. (2017). A Doublet-Lattice Method Correction Approach for High Fidelity Gust Loads Analysis. In *58th AIAA/ASCE/AHS/ASC Structures, Structural Dynamics, and Materials Conference*, 9 -13 January 2017. Grapevine, Texas. ISBN 978-1-62410-453-4, pp. 1–17. doi:10.2514/6.2017-0632.

[14] Johnson, E. H. and Rodden, W. P. (1994). *MSC Nastran Version 68 Aeroelastic Analysis User's Guide*. ISBN 0369111222.

[15] Easa (2007). Certification Specifications for Large Aeroplanes CS-25. Tech. Rep. 19 September.

[16] Jones, D. and Gaitonde, A. Future Fast Methods for Loads Calculations : The FFAST Project. In *Innovation for Sustainable Aviation in a Global Environment proceedings of Aerodays*. pp. pp. 110–115.

[17] Valente, C., Jones, D., Gaitonde, A., et al. (2015). OpenFSI Interface For Strongly Coupled Steady And Unsteady Aeroelasticity. In *IFASD 2015 International Forum on Aeroelasticity and Strucutral Dynamics*. Saint Petersburg, Russia, pp. 1–16.

[18] Schwamborn, D., Gerhold, T., and Heinrich, R. (2006). The DLR TAU-Code: Recent Applications in Research and Industry. *European Conference on Computational Fluid Dynamics, ECCOMAS CFD 2006*, 1–25.

[19] Heinrich, R. and Reimer (2013). Comparison of different approaches for gust modeling in the CFD code TAU. In *IFASD 2013 International Forum on Aeroelasticity and Structural Dynamics*. Bristol, UK, pp. 1–12.

[20] Jeyakumar, G. and Jones, D. (2013). Aerofoil gust responses in viscous flows using prescribed gust velocities. Tech. rep.

[21] Wales, C., Jones, D., and Gaitonde, A. (2014). Prescribed Velocity Method for Simulation of Aerofoil Gust Responses. *Journal of Aircraft*, 1–13. ISSN 0021-8669. doi:10.2514/1.C032597.

[22] DLR German Aerospace Center. 4th AIAA CFD Drag Prediction Workshop.

[23] Klimmek, T. (2013). Development of a Structural Model of the CRM Configuration for Aeroelastic and Loads Analysis. In *IFASD2013 International Forum on Aeroelasticity and Structural Dynamics*. doi:10.3293/asdj.2014.27.

[24] Allmaras, S. R., Johnson, F. T., and Spalart, P. R. (2012). Modifications and clarifications for the implementation of the Spalart-Allmaras turbulence model. *Seventh International Conference on Computational Fluid Dynamics*, (ICCFD7-1902).

[25] DLR German Aerospace Center. DLR coarse mesh for 4th Drag prediction workshop.

COPYRIGHT STATEMENT